

Case Studies of Photospheric Magnetic Field Properties of Active Regions Associated with X-class Solar Flares

(Kajian Kes Sifat Medan Magnet Fotosfera Rantau Aktif dikaitkan dengan Suar Matahari Kelas X)

WAI-LEONG TEH* & FARAHANA KAMARUDIN

ABSTRACT

Solar flares are a transient phenomenon occurred in the active region (AR) on the Sun's surface, producing intense emissions in EUV and soft X-ray that can wreak havoc in the near-Earth space mission and satellite as well as radio-based communication and navigation. The ARs are accompanied with strong magnetic fields and manifested as dark spots on the photosphere. To understand the photospheric magnetic field properties of the ARs that produce intense flares, two ARs associated with X-class flares, namely AR 12192 and AR 12297, occurred respectively on 25 October 2014 and 11 March 2015, are studied in terms of magnetic classification and various physical magnetic parameters. Solar images from the Langkawi National Observatory (LNO) and physical magnetic parameters from the Space-weather HMI Active Region Patches (SHARP) are used in this study. A total of seven SHARP magnetic parameters are examined which are calculated as sums of various magnetic quantities and have been identified as useful predictors for flare forecast. These two ARs are classified as $\beta\gamma\delta$ sunspots whereas their formation and size are quite different from each other. Our results showed that the intensity of a flare has little relationship with the area of an AR and the magnetic free energy; and the temporal variation of individual magnetic parameter has no obvious and consistent pre-flare feature. It is concluded that the temporal variation of individual magnetic parameter may not be useful for predicting the onset time of a flare.

Keywords: Active region; photospheric magnetic field; solar flare

ABSTRAK

Suar suria ialah satu fenomena yang berlaku di rantau aktif permukaan Matahari dengan menghasilkan pancaran peramalan dalam EUV dan sinar-X lembut yang boleh memberikan kesan kepada misi angkasa lepas-bumi dan satelit serta komunikasi berasaskan radio dan navigasi. Rantau aktif ini mempunyai medan magnet yang kuat dan dimanifestasikan sebagai tompok gelap pada permukaan fotosfera Matahari. Bagi memahami ciri medan magnet di lapisan fotosfera, dua kawasan rantau aktif iaitu daripada AR 12192 dan AR 12297 yang telah menghasilkan suar suria kelas X pada 25 Oktober 2014 dan 11 Mac 2015 telah dikaji dalam penyelidikan ini bagi meneliti pengelasan magnet dan pelbagai parameter fizikal magnet. Imej Matahari dari Observatori Negara Langkawi dan parameter fizikal magnet dari Space-weather HMI Active Region Patches (SHARP) telah digunakan dalam kajian ini. Sebanyak tujuh parameter magnet dari SHARP dianalisis dan parameter ini telah dikenal pasti dapat membantu dalam peramalan suar suria. Kedua-dua rantau aktif ini dikelaskan dalam tompok matahari berkelas $\beta\gamma\delta$ sedangkan pembentukan dan saiz kedua-dua rantau ini agak berbeza antara satu sama lain. Hasil penyelidikan menunjukkan keamatan suar suria mempunyai sedikit hubungan dengan kawasan rantau aktif dan tenaga bebas magnet serta perubahan parameter magnet bagi setiap rantau aktif tidak mempunyai ciri awalan pancaran yang jelas dan tekal. Dengan itu, dapat disimpulkan bahawa perubahan parameter magnet individu mungkin tidak boleh digunakan sebagai salah satu ciri dalam peramalan permulaan suar.

Kata kunci: Medan magnet fotosfera; rantau aktif; suar suria

INTRODUCTION

Solar flares are a transient phenomenon that lasts from tens of minutes to hours, releasing intense emissions in EUV and soft X-ray. The typical amount of energy released from a flare is about 10^{32} erg, which can wreak havoc in the

near-Earth space mission and satellite as well as radio-based communication and navigation. The intensity of a flare is based on the soft X-ray (SXR) peak flux measured by the GOES satellite. For example, the SXR peak fluxes of X-class flares are equal to or larger than 1.0×10^{-4} Wm⁻²,

which are considered as largest flares. Intense flares usually occur in the ARs on the Sun's surface, manifested as dark spots on the photosphere. The ARs are accompanied with strong magnetic fields and a lower temperature than the surrounding region.

ARs are classified by the magnetic configurations of sunspot groups, e.g. the Mount Wilson magnetic classification scheme. Observations showed that δ sunspots, where umbrae of both positive and negative polarities are embedded within a single penumbra, have a high potential to produce intense flares (Guo et al. 2014; Sammis et al. 2000; Teh 2019; Yang et al. 2017). Sammis et al. (2000) found that $\beta\gamma\delta$ sunspots with area greater than 1000 mH (micro-hemisphere) had $\sim 40\%$ probability to produce X-class flares.

In addition to the magnetic complexity and size of ARs, previous studies indicated that the flare productivity of ARs has a good relationship with the photospheric magnetic field properties, e.g. magnetic helicity (Tian et al. 2005; Török & Kliem 2005), high-gradient polarity inversion line (PIL) (Schrijver 2007), magnetic free energy (Jing et al. 2010; Leka & Barnes 2007; Su et al. 2014), and magnetic shear angle (Hagyard et al. 1984; Leka & Barnes 2007). However, the individual magnetic property of an AR (e.g. magnetic helicity and magnetic free energy) has little ability to distinguish the flaring AR from the flare-quiet one (Leka & Barnes 2003).

Photospheric magnetic field and associated magnetic field properties have been widely implemented for flare forecasts with machine-learning algorithms (Bobra & Couvidat 2015; Liu et al. 2017). Bobra and Couvidat (2015) for the first time used a large data set of photospheric vector magnetic fields measured by the Helioseismic and Magnetic Imager (HMI) (Schou et al. 2012) onboard the Solar Dynamics Observatory (SDO) (Pesnell et al. 2012) and associated magnetic field properties to perform flare predictions with the support vector machine algorithm. They found 13 SHARP magnetic parameters to be good predictors for flares. Later, Teh (2019) showed that there are good correlations among seven magnetic parameters out of the 13 magnetic parameters. These seven magnetic parameters are listed in Table 1, with their descriptions and formulae. Moreover, Teh (2019) obtained a threshold for low bound for each of the seven magnetic parameters and found that $\sim 77\%$ of X-class flares occur within 7 days after the time when the thresholds of all the magnetic parameters but TOTBSQ are met.

With the aim of understanding the photospheric magnetic field properties of ARs that produce intense flares, two ARs associated with X-class flares, namely AR 12192 and AR 12297, are studied in terms of magnetic classification and various physical magnetic parameters. A total of seven SHARP magnetic parameters obtained by

Teh (2019) are used to examine the temporal variation of individual magnetic parameter before and after the flare started.

MATERIALS AND METHODS

GROUND AND SATELLITE DATA

Two data sets were used in this study, namely, the LNO data and the SHARP data derived from SDO/HMI (Bobra et al. 2014; Hoeksema et al. 2014). The LNO data are the solar images observed by the solar telescope with three different filters for white light, Hydrogen alpha ($H\alpha$), and Calcium K-line (Cak). The white light filter transmits the entire visible spectrum of light but attenuates it to a safe observing level, allowing the sunspots on the photosphere of the Sun to be observed. Therefore, the white light images are commonly used for sunspot number calculation (Kamarudin et al. 2017). $H\alpha$ and Cak filters are the narrowband filters, transmitting specific wavelengths of light at 395.0 and 656.3 nm, respectively, suitable to observe the solar filaments and prominences. The SHARP data consist of the magnetic field parameters of an AR, calculated from the photospheric vector magnetic field or line-of-sight (LoS) magnetic field observed by the HMI instrument onboard the SDO spacecraft, throughout its transit time on the visible solar disk. The SHARP data are at 12-min cadence and based on the heliographic cylindrical equal-area coordinates. Seven magnetic parameters are implemented in this study, as listed in Table 1. They are the total unsigned magnetic flux (USFLUX), total unsigned vertical current (TOTUSJZ), total unsigned current helicity (TOTUSJH), sum of flux near PIL (R_VALUE), total photospheric magnetic free energy density (TOTPOT), total magnitude of Lorentz force (TOTBSQ), and area of AR (AREA_ACR), which have been identified as useful predictors for flare forecasting (Teh 2019). For the detailed descriptions of the seven magnetic parameters, the reader can find it in the paper of Bobra et al. (2014) and the references therein. Note that the most valuable predictors for flare forecasting were calculated as sums, rather than means, of various physical quantities (Bobra & Couvidat 2015). Liu et al. (2017) found that TOTUSJH, TOTUSJZ, and R_VALUE are the most important parameters for classifying flaring ARs into different classes.

MAGNETIC CLASSIFICATION SCHEME OF SUNSPOTS

Sunspots appear on the solar disk as individual spots or as a group of spots, with various formations and sizes. In this paper, the Mount Wilson scheme is used to classify sunspot groups. There are five major classes of sunspot groups, i.e. α , β , γ , $\beta\gamma$, and δ . Their descriptions are summarized in Table 2. According to their magnetic

complexity, α , β , and γ are the simple sunspots, while $\beta\gamma$ and δ are the intermediate ones. The complex ones can be the combination of $\beta\gamma$ and δ ($\beta\gamma\delta$) or γ and δ ($\gamma\delta$). To perform the sunspot classification, the white light image and the photospheric magnetogram are needed. The white light image is to distinguish the umbra (in dark) and penumbra (in gray) of the sunspot, while the photospheric magnetogram is to identify the magnetic polarity of the sunspots and the high-gradient polarity inversion line (PIL), which is the boundary between the positive and negative polarities of the sunspots. According to the sunspot group descriptions in Table 2, the sunspot configuration can then be classified.

RESULTS AND DISCUSSION

Two X-class solar flares were studied in this paper. The first flare event happened in the AR 12192 on October 25, 2014, with a SXR peak flux at X1.0 level. The start, peak, and end times of the flare were at 16:55 UT, 17:08 UT, and 18:11 UT, respectively. The duration of the flare was about 76 min. Figure 1 shows the LNO solar images of AR 12192 for white light, H α , and Cak filters, taken at different UT times. Those observations were made prior to the start time of the flare. In the white light and Cak images, the umbra (dark) and penumbra (gray) of the sunspots are clearly resolved, while the H α image indicates that a solar filament is formed within the AR. Figure 2 shows the photospheric magnetogram of AR 12192 at 12:36 UT, where the red and blue color codes denote the positive and negative polarities of magnetic fields, respectively. Note that the color scale represents the strength of the magnetic field and it is omitted. The positive/negative polarity indicates the magnetic field lines pointing toward/away from the observer. According to the white light image of AR 12192, one can classify the region enclosed by the circle in Figure 2 as δ sunspots, where both positive and negative polarities of umbrae are embedded within the same penumbra. Furthermore, Figure 2 indicates that the AR 12192 consists of bipolar sunspot groups accompanied with more than one PIL as marked by the magenta dashed lines. Therefore, the AR 12192 is classified as $\beta\gamma\delta$ sunspots.

The second flare event happened in the AR 12297 on March 11, 2015, with a SXR peak flux at X2.1 level. The start, peak, and end times of the flare were at 16:11 UT, 16:22 UT, and 16:29 UT, respectively. The duration of the flare was about 18 min. Figure 3 shows the LNO solar images for AR 12297, with the same format as Figure 1. Those observations were made before the flare started. Two remarks are that the sunspots of AR 12297 are not much scattered; and a W-shape filament is formed inside the AR (Figure 3(b)). Figure 4 shows the photospheric magnetogram of AR 12297 at 09:36 UT. It is found that (1) the δ sunspots are embedded within the AR, as $\beta\gamma\delta$

marked by the circle in Figure 4; and (2) the AR 12297 is of $\beta\gamma\delta$ sunspots.

Figures 5 and 6 show the time series of seven SHARP magnetic parameters for AR 12192 and AR 12297 to examine their magnetic field evolution. The data duration is 24 h and the green, red, and cyan vertical lines in the figure denote the start, peak, and end times of the flare, respectively. Figure 5(c) shows that from 00:00 UT onward, the area of AR 12192 started to grow until around 09:00 UT, and then decreased to a more or less stable level lasted for ~ 7 h. Finally, it gradually decreased right after the flare started. The other six magnetic parameters were also increasing during the first ~ 6 h of the AR growing and then decreasing at the time before the AREA_ACR decreased. During ~ 11 h before flaring, the variations of TOTUSJH, TOTUSJZ, R_VALUE, and TOTBSQ were dramatic as compared to USFLUX, TOTPOT, and AREA_ACR.

On the AR 12297, Figure 6(c) shows that the area of the AR was growing rapidly from 00:00 UT to 06:00 UT, and then reached a more or less stable level for ~ 6 h; later it gradually increased till the flare started. During ~ 7 h before the flaring, the variations of TOTUSJZ, USFLUX, and R_VALUE were more dramatic than TOTUSJH, TOTPOT, AREA_ACR, and TOTBSQ.

These two X-class (X1.0 and X2.1) flares are produced by the $\beta\gamma\delta$ sunspots. However, the formation and size of these two ARs are quite different, where AR 12192 is much scattered and larger than AR 12297. Despite the small size of AR, AR 12297 can produce a large flare. This result is consistent with the finding by Teh (2019) that the intensity of a flare has little relationship with the area of the AR. The flare intensity has been considered to be related with the accumulated magnetic free energy released by magnetic reconnection (Jing et al. 2010; Su et al. 2014; Yang et al. 2017). This magnetic free energy is partly related to TOTPOT. As shown in Figures 5(c) and 6(c), TOTPOT is larger in AR 12192 than in AR 12297. Therefore, TOTPOT may not be a significant factor to determine the flare intensity. This result can be interpreted by the energy partition in a flare (Emslie et al. 2004; Reeves et al. 2010). Since magnetic reconnection converts the accumulated magnetic free energy into thermal energy, conduction, and radiation, how the energy partition is made for thermal energy is a key factor to power a flare.

By inspecting the magnetic field properties of the AR at the time when the flare started, no obvious and consistent pre-flare features can be found among the seven magnetic parameters. For example, the X1.0 flare occurred around the peak of TOTUSJH and the dip of TOTUSJZ (Figure 5(a)), but the X2.1 flare happened around the dip of TOTUSJH and the peak of TOTUSJZ instead (Figure 6(a)). Similar results can also be found in the USFLUX and R_VALUE of the two ARs. While

both the two flares happened during the raising phase of TOTPOT and TOTBSQ, no clear pattern is found for them; the same conclusion is reached for AREA_ACR. Therefore, the temporal variation of individual magnetic parameter may not be useful for predicting the onset time of a flare. This result implies that the factors to trigger solar flares are complex and cannot be solely determined by using a single magnetic property of the AR. Notably, our finding agrees with the previous studies by Bobra and Couvidat (2015) and Liu et al. (2017), for which they used more than ten magnetic field parameters to train the machine-learning algorithm and to predict the flaring ARs. Teh (2019) has pointed out that the necessary condition

to produce an intense flare is that the strengths of the seven magnetic parameters have built up and reached above their thresholds, but the sufficient condition is the triggering mechanism of flares. Note that the strengths of the seven magnetic parameters at the time of flaring for these two studied events are larger than their thresholds obtained by Teh (2019). Various onset mechanisms of flares have been proposed in the literature, e.g. emerging flux on PIL (Feynman & Martin 1995; Moore et al. 2001), reversed magnetic shear (Kusano et al. 2004), and small magnetic disturbances (Bamba et al. 2013; Kusano et al. 2012). These onset mechanisms determine when an AR will produce a flare.

TABLE 1. Seven SHARP magnetic parameters and formulae

Keyword	Description	Formula*
TOTUSJH	Total unsigned current helicity	$H_{c\text{total}} \propto \sum B_z \cdot J_z $
TOTBSQ	Total magnitude of Lorentz force	$F \propto \sum B^2$
TOTPOT	Total photospheric magnetic free energy density	$\rho_{\text{tot}} \propto \sum (\mathbf{B}^{\text{Obs}} - \mathbf{B}^{\text{Pot}})^2 dA$
TOTUSJZ	Total unsigned vertical current	$J_{z\text{total}} = \sum J_z dA$
USFLUX	Total unsigned flux	$\Phi = \sum B_z dA$
AREA_ACR	Area of strong field pixels in the AR	Area = $\sum \text{Pixels}$
R_VALUE	Sum of flux near polarity inversion line	$\Phi = \sum B_{\text{Los}} dA$

*Refer to Bobra et al. (2014) for details

TABLE 2. Five major classes of sunspot groups

Class	Description
α	A single dominant sunspot with either a positive or a negative polarity
β	A pair of dominant sunspots of opposite polarity with a simple polarity inversion line
γ	Complex groups with irregular distribution of polarities
$\beta\gamma$	Bipolar groups with more than one polarity inversion line
δ	Umbræ of opposite polarity together in a single penumbra

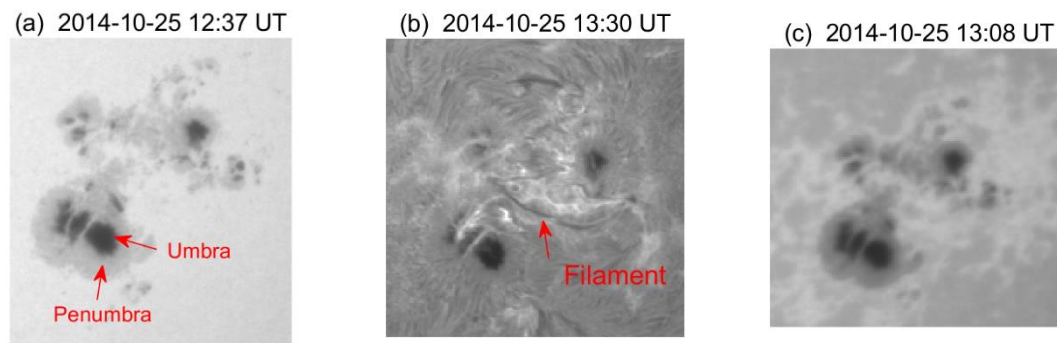


FIGURE 1. LNO solar images of AR 12192 for (a) white light, (b) H_{α} , and (c) Ca_k filters, taken at different UT times

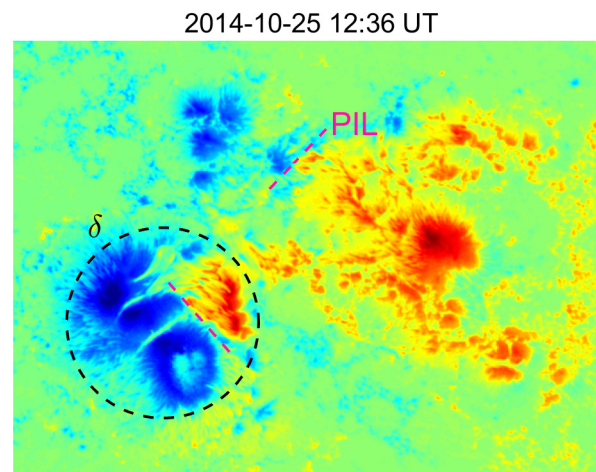


FIGURE 2. SHARP magnetogram of AR 12192. The red and blue denote the positive and negative polarities of magnetic fields, respectively

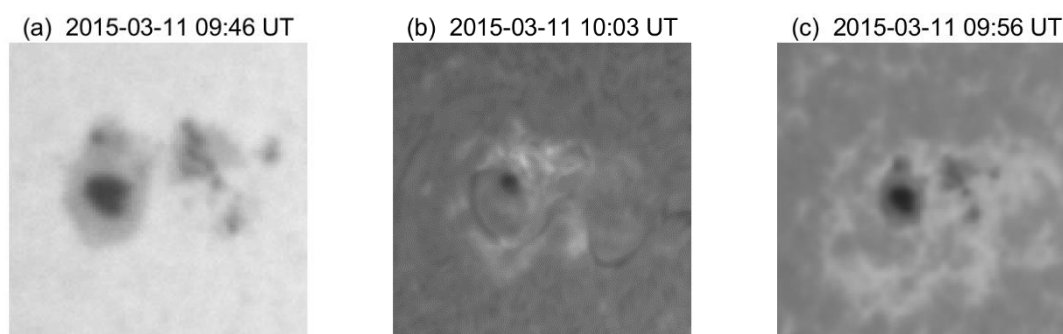


FIGURE 3. LNO solar images of AR 12297 for (a) white light, (b) H_{α} , and (c) Ca_k filters, taken at different UT times

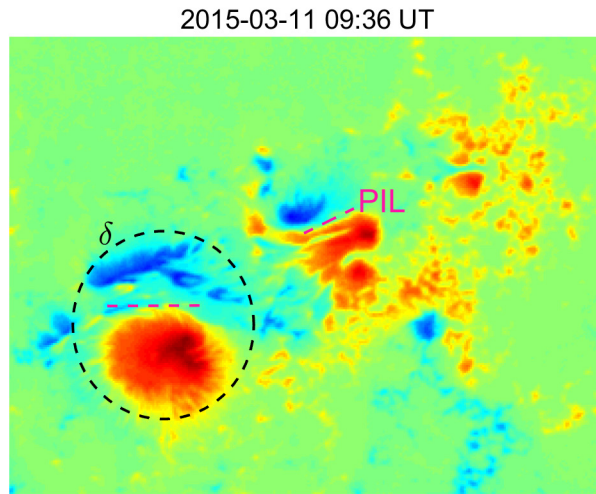


FIGURE 4. SHARP magnetogram of AR 12297. The red and blue denote the positive and negative polarities of magnetic fields, respectively.

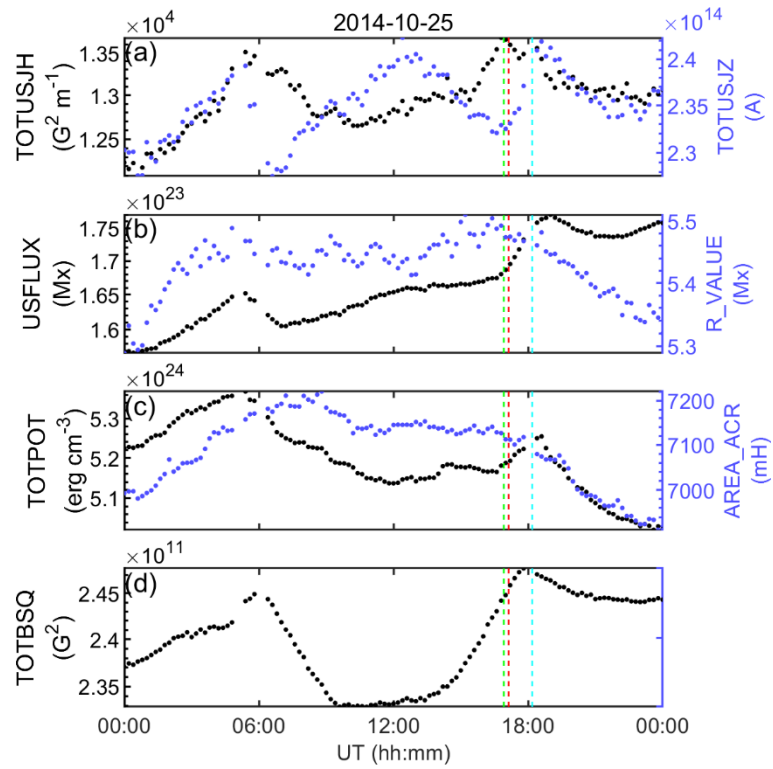


FIGURE 5. Time series of seven SHARP magnetic parameters observed in AR 12192 on 25 October 2014. The green, red, and cyan dashed lines denote the start, peak, and end times of the flare

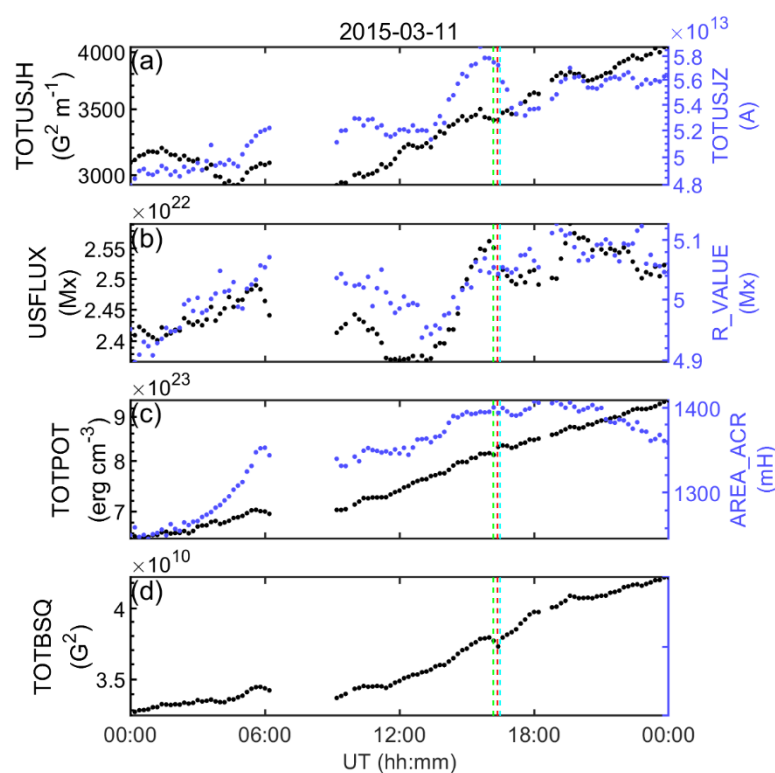


FIGURE 6. Time series of seven SHARP magnetic parameters observed in AR 12297 on 11 March 2015, with the same format as Figure 5

CONCLUSION

The photospheric magnetic field properties of two ARs associated with X-class flares have been examined in terms of magnetic classification and various magnetic field parameters derived from SDO/HMI. These two ARs are identified as $\beta\gamma\delta$ sunspots whereas their formation and size are quite different from each other. It is found that the intensity of a flare has a weak relationship with the area of an AR and the magnetic free energy; and the temporal variation of individual magnetic parameter has no obvious and consistent pre-flare feature. It is concluded that the temporal variation of individual magnetic parameter may not be useful for predicting the onset time of a flare. A comprehensive statistical study on this topic can further advance our understanding of the solar flares.

ACKNOWLEDGEMENTS

This work was supported by the grant of Universiti Kebangsaan Malaysia (GUP-2018-086). The SHARP vector magnetic fields and associated magnetic parameters can be downloaded at http://jsoc.stanford.edu/ajax/lookdata.html?ds=hmi.sharp_cea_720s and the integrated

Lorentz force data at <http://jsoc.stanford.edu/ajax/lookdata.html?ds=cgem.lorentz>.

REFERENCES

- Bamba, Y., Kusano, K., Yamamoto, T.T. & Okamoto, T.J. 2013. Study on the triggering process of solar flares based on Hinode/SOT observations. *The Astrophysical Journal* 778(1): 48-61.
- Barnes, G. & Leka, K.D. 2006. Photospheric magnetic field properties of flaring versus flare-quiet active regions. III. Magnetic charge topology models. *The Astrophysical Journal* 646(2): 1303-1318.
- Bobra, M.G. & Couvidat, S. 2015. Solar flare prediction using SDO/HMI vector magnetic field data with a machine-learning algorithm. *The Astrophysical Journal* 798(2): 135-146.
- Bobra, M.G., Sun, X., Hoeksema, J.T., Turmon, M., Liu, Y., Hayashi, K., Barnes, G. & Leka, K.D. 2014. The helioseismic and magnetic imager (HMI) vector magnetic field pipelines: SHARPs - space-weather HMI active region patches. *Solar Physics* 289(9): 3549-3578.
- Emslie, A.G., Kucharek, H., Dennis, B.R., Gopalswamy, N., Holman, G.D., Share, G.H., Vourlidas, A., Forbes, T.G., Gallagher, P.T., Mason, G.M. & Metcalf, T.R. 2004.

- Energy partition in two solar flare/CME events. *Journal of Geophysical Research: Space Physics* 109(A10): 1-15.
- Feynman, J. & Martin, S.F. 1995. The initiation of coronal mass ejections by newly emerging magnetic flux. *Journal of Geophysical Research: Space Physics* 100(A3): 3355-3367.
- Gou, J., Lin, J.B. & Deng, Y.Y. 2014. The dependence of flares on the magnetic classification of the source regions in solar cycles 22-23. *Monthly Notices of the Royal Astronomical Society* 441(13): 2208-2211.
- Hagyard, M.J., Smith, J.B., Teuber, D. & West, E.A. 1984. A quantitative study relating observed shear in photospheric magnetic fields to repeated flaring. *Solar Physics* 91(1): 115-126.
- Hoeksema, J.T., Liu, Y., Hayashi, K., Sun, X., Schou, J., Couvidat, S., Norton, A., Bobra, M., Centeno, R., Leka, K.D. & Barnes, G. 2014. The helioseismic and magnetic imager (HMI) vector magnetic field pipeline: overview and performance. *Solar Physics* 289(9): 3483-3530.
- Jing, J., Tan, C., Yuan, Y., Wang, B., Wiegmann, T., Xu, Y. & Wang, H. 2010. Free magnetic energy and flare productivity of active regions. *The Astrophysical Journal* 713(1): 440-449.
- Kamarudin, F., Tahar, M.R., Saibaka, N.R. & Padang, L.A.L. 2017. Relative sunspot number observed from 2013 to 2015 at Langkawi National Observatory. *Advanced Science Letters* 23(2): 1285-1288.
- Kusano, K., Bamba, Y., Yamamoto, T.T., Iida, Y., Toriumi, S. & Asai, A. 2012. Magnetic field structures triggering solar flares and coronal mass ejections. *The Astrophysical Journal* 760(1): 31-40.
- Kusano, K., Maeshiro, T., Yokoyama, T. & Sakurai, T. 2004. The trigger mechanism of solar flares in a coronal arcade with reversed magnetic shear. *The Astrophysical Journal* 610(1): 537-549.
- Leka, K.D. & Barnes, G. 2007. Photospheric magnetic field properties of flaring versus flare-quiet active regions. IV. A statistically significant sample. *The Astrophysical Journal* 656(2): 1173-1186.
- Leka, K.D. & Barnes, G. 2003. Photospheric magnetic field properties of flaring versus flare-quiet active regions. II. Discriminant analysis. *The Astrophysical Journal* 595(2): 1296-1306.
- Liu, C., Deng, N., Wang, J.T. & Wang, H. 2017. Predicting solar flares using SDO/HMI vector magnetic data products and the random forest algorithm. *The Astrophysical Journal* 843(2): 104-118.
- Moore, R.L., Sterling, A.C., Hudson, H.S. & Lemen, J.R. 2001. Onset of the magnetic explosion in solar flares and coronal mass ejections. *The Astrophysical Journal* 552(2): 833-848.
- Pesnell, W.D., Thompson, B. & Chamberlin, P. 2012. The solar dynamics observatory (SDO). In *The Solar Dynamics Observatory*, edited by Chamberlin, P., Pesnell, W.D. & Thompson, B. New York: Springer. 275: 3-15.
- Reeves, K.K., Linker, J.A., Mikić, Z. & Forbes, T.G. 2010. Current sheet energetics, flare emissions, and energy partition in a simulated solar eruption. *The Astrophysical Journal* 721(2): 1547-1558.
- Sammis, I., Tang, F. & Zirin, H. 2000. The dependence of large flare occurrence on the magnetic structure of sunspots. *The Astrophysical Journal* 540(1): 583-587.
- Schou, J., Scherrer, P.H., Bush, R.I., Wachter, R., Couvidat, S., Rabello-Soares, M.C., Bogart, R.S., Hoeksema, J.T., Liu, Y., Duvall, T.L. & Akin, D.J. 2012. Design and ground calibration of the helioseismic and magnetic imager (HMI) instrument on the solar dynamics observatory (SDO). *Solar Physics* 275(1-2): 229-259.
- Schrijver, C.J. 2007. A characteristic magnetic field pattern associated with all major solar flares and its use in flare forecasting. *The Astrophysical Journal Letters* 655(2): L117-L120.
- Su, J.T., Jing, J., Wang, S., Wiegmann, T. & Wang, H.M. 2014. Statistical study of free magnetic energy and flare productivity of solar active regions. *The Astrophysical Journal* 788(2): 150-160.
- Teh, W.L. 2019. A statistical study of photospheric magnetic field properties of active regions associated with M- and X-class flares using SDO/HMI vector magnetic field data. *Journal of Atmospheric and Solar-Terrestrial Physics* 188: 44-51.
- Tian, L.R., Alexander, D., Liu, Y. & Yang, J. 2005. Magnetic twist and writhe of δ active regions. *Solar Physics* 229(1): 63-77.
- Török, T. & Kliem, B. 2005. Confined and ejective eruptions of kink-unstable flux ropes. *The Astrophysical Journal Letters* 630(1): L97-L100.
- Yang, Y.H., Hsieh, M.S., Yu, H.S. & Chen, P.F. 2017. A statistical study of flare productivity associated with sunspot properties in different magnetic types of active regions. *The Astrophysical Journal* 834(2): 150-161.
- Wai-Leong Teh*
Space Science Centre
Institute of Climate Change
Universiti Kebangsaan Malaysia
43600 UKM Bangi, Selangor Darul Ehsan
Malaysia
- Farahana Kamarudin
Langkawi National Observatory
Malaysian Space Agency
Empangan Bukit Malut
07000 Langkawi, Kedah Darul Aman
Malaysia

*Corresponding author; email: wtch@ukm.edu.my

Received: 17 March 2020

Accepted: 12 June 2020